Quantum Walk of Rydberg Atoms Embedded in Photonic Crystal

A Thesis

submitted to

Indian Institute of Science Education and Research, Pune

in partial fulfillment of the requirements for the

BS-MS Dual Degree Programme

by

Jugal Talukdar

(Registration Number: 20121108)

Indian Institute of Science Education and Research, Pune

Dr. Homi Bhabha Road,

Pashan, Pune 411008, INDIA.

April, 2017

Supervisor: **Dr. Rejish Nath**

Certificate

This is to certify that this dissertation entitled **Quantum Walk of Rydberg Atoms Embedded in Photonic Crystal** towards the partial fulfilment of the BS-MS dual degree programme at the Indian Institute of Science Education and Research, Pune represents study/work carried out by **Jugal Talukdar** under the supervision of **Dr. Rejish Nath**, Assistant Professor, Department of Physics , during the academic year 2016-2017.

Dr. Rejish Nath

Jugal Talukdar

Committee:

Dr. Rejish Nath

Dr. TS Mahesh

This thesis is dedicated to *Maa, Deuta, Mama and Kan*

Declaration

I hereby declare that the matter embodied in the report entitled **Quantum Walk of Rydberg Atoms Embedded in Photonic Crystal** are the results of the work carried out by me at the Department of Physics, Indian Institute of Science Education and Research, under the supervision of **Dr. Rejish Nath** and the same has not been submitted elsewhere for any other degree.

Jugal Talukdar

Dr. Rejish Nath

Acknowledgments

Foremost, I would like to express my deepest thanks and heartfelt gratitude to my supervisor, Dr. Rejish Nath for his sincere guidance and constructive discussions, without which this thesis would not have been possible. I will forever be indebted to him for the zeal and motivation he has imbibed in me which will help me in my career ahead.

I am very thankful to my TAC member, Dr. T.S. Mahesh for his valuable suggestions.

I am extremely grateful to my group members Chinmayee, Yashwant, Ankita, Supriti, Banibrata and Sagarika for their suggestions, support and maintaining a jovial atmosphere. I am particularly thankful to Chinmayee for the help she has extended in finalizing the various aspects of this thesis and Yashwant, for the insightful discussions.

I take immense pleasure in extending my gratitude to Prof. K.N. Ganesh, Director, IISER Pune for such a wonderful opportunity. I also thank all the teaching and non-teaching staff of the Physics department for their help and cooperation at various stages of my project.

I am grateful for the handful of friends, in and out of campus who has been with me through thick and thin and my family members for their love and support.

Lastly, I would like to dedicate this thesis to my parents for their unconditional love and undying support in every aspect of my life.

Abstract

The subject of this thesis is the theoretical investigation of an atomic chain of Rydberg atoms embedded in a photonic crystal waveguide. Atoms coupled to the photonic crystal show prodigious coherent and dissipative dynamics. In coherent regime, the atoms interact via the evanescent fields resulting in correlated many-body dynamics which demands powerful numerical tool for modelling. The first part of the thesis deals with the excitation dynamics of Rydberg atoms in optical lattice. The excitation dynamics of a Rydberg atomic chain differ significantly from single atom dynamics due to the phenomenon of Rydberg blockade. Additionally, the number of excitations in the Rydberg atomic chain depends strongly on the detuning from resonance which leads to dynamical crystallisation. In the second part we study an atomic chain embedded in photonic crystal waveguide with atomic frequency highly detuned from the photonic band edge frequency. Here, due to the presence of band gap, a coherent hopping of Rydberg excitations takes place in the atomic chain. This coherent many-body interaction is designed appropriately to facilitate controlled hopping along the atomic chain which emulates quantum walk dynamics.

Contents

List of Figures

Chapter 1

Introduction

The field of quantum information science is fuelled by a wide range of scientific opportunities in quantum computation[1, 2] and quantum communication[3] among other emerging fields[4]. The field is boosted by quantum networks which consists of quantum nodes and quantum channels. The quantum nodes generate and store quantum information which is transferred via the quantum channels. However, a quantum network can also be thought of as a quantum simulator. Quantum simulator enables us to investigate quantum many-body phenomena[5, 6, 7, 8] emerging due to interactions between the quantum nodes[9, 10]. Quantum networks can be realised physically using systems which can efficiently generate and store quantum memories, and are capable of transferring the stored information across the network.

Photons can carry quantum information over long distances whereas atoms can store this information, thereby making atom-light interaction an ideal tool to investigate quantum networking. Interaction between light and matter in free space[11] has been studied widely. However when an atomic ensemble is confined to cavity or embedded in a dielectric environment, a window to new regimes of dissipative dynamics gets opened[12, 13, 14]. Along with the modification of dissipative dynamics, such dielectric environment can be used to manipulate atom-atom interactions, which leads to atomic dynamics very different from the dynamics in free space[15]. Depending on the properties of the atom, its interaction with photonic mode is manipulated in order to design interesting dynamics[16].

In recent years efforts have been made to integrate nano-photonics and atomic physics. It provides us with a powerful tool to look at the quatum transport in a new light[17].

Photonic systems provide a tool for controllable light-matter interaction at the level of single photon[18, 19, 20]. The systems coupled to nanophotonic structure have been studied in the coherent regime as well as in the dissipative regime[21, 22]. Engaging research in this area can pave way for future experimental works.

Additionally, working with Rydberg atoms can be further enriching as Rydberg atoms exhibit remarkable properties[23] such as long radiative lifetimes and a huge dipole moment among other properties. Moreover, an ensemble of Rydberg atoms gives rise to the phenomenon of Rydberg blockade, a strong interaction which prevents a new excitation in a finite volume[24, 25, 26]. Key point here is that Rydberg atoms provide unique ability to control the interaction strength over a wide range. For this reason Rydberg physics finds wide applications from quantum information processing, quantum optics, BEC physics to plasma physics[27, 28, 29, 30, 31, 32, 33].

In our work we focus on coupling a Rydberg atomic chain trapped in photonic crystal waveguide. The motivation to work along this direction is enhanced by the studies which show the strong coupling mediated by nano photonic environment for a solid state system[34]. Moreover, similar regime of coupling has been demonstrated using cold atom setups[35, 36, 37, 38]. Single atoms have been coupled to photonic crystal via local imperfections[37, 38]. We show that if an atomic chain of Rydberg atoms is made to interact via the evanescent guided modes of photonic crystal waveguide, it leads to an excitation manifold based outcome which can play vital role in quantum computation and quantum information processing. Thus our system can be used as a potential tool to realise controlled light-matter interaction, thereby depicting the impact of photonic crystal in quantum many-body physics.

1.1 Outline of this work

This thesis is organized as follows:

Chapter 2 summarises the basic concepts of Rydberg physics and photonic crystal waveguide. First a detailed discussion on the properties of Rydberg atom is included. We then explain the structure and foundations of photonic crystal by relating it to atomic crystal lattice. Finally, quantum walk dynamics is discussed briefly. We have focussed mainly on continuous-time quantum walk and thereby discussed mathematically the transition from its classical analog.

Chapter 3 is about the dynamics of Rydberg atoms under external fields. We start with single atom dynamics, before discussing collecting many-body dynamics of Rydberg atoms. Thereafter, a detailed study of a Rydberg atomic chain in the weak coupling limit where detuning can be used as a parameter to tune the excitation manifolds is provided.

Chapter 4 deals with an atomic chain of Rydberg atoms embedded to photonic crystal waveguide. The atomic transition frequency of the atom is highly detuned from the band edge frequency of the photonic crystal w.r.t which coupling of the atoms to the photonic modes is considered. We then derive the interaction Hamiltonian and the length parameter which dictates the restriction of exchange of excitation along the atomic chain. The effect of the photonic modes can be understood in dyadic green function perspective explaining the response of the atoms in the photonic crystal waveguide. Thus, we show how the Hamiltonian can be expressed in terms of Green function.

Chapter 5 is dedicated to the coherent dynamics of a specific case of excitation manifolds which is single excitation in the atomic chain. We consider two initial conditions, an excited atom exactly in the middle of the atomic chain (symmetric) and somewhere other than the middle position (asymmetric). We discuss the dynamics shown by the excitation for both the cases. The spread of the excitation is calculated and from its linear dependence on time we show that the single excitation in the atomic chain is indeed a quantum walker.

Chapter 6 briefly summarises the results of the previous chapters and gives an overview of the work in progress.

Chapter 2

Basic concepts

This chapter deals with the basic physical concepts related to our work. We have focused particularly on Rydberg atoms and photonic crystal waveguide. Section 2.1 has the details of the properties and interactions of Rydberg atoms. We discuss the interactions of the Rydberg atoms in an ensemble. In Section 2.2, it is discussed about the photonic crystal, and the behaviour of trapped atoms near the photonic crystal waveguide. The basic idea of quantum walk is discussed in section 2.3. Here we give importance to continuous-time walk and explain the expected behaviour of a quantum walker.

2.1 Rydberg atom

Rydberg atoms are atoms with one or more electrons in the excited states which have very high principal quantum number. It shows many exaggerated properties as a response to electro-magnetic field. As excited states are far away from the nucleus, quantum defect has to be considered .

$$E_n = -\frac{R_y}{(n - \delta_{njl})^2} \tag{2.1}$$

Where δ_{njl} is the quantum defect and R_y is the Rydberg constant. Quantum defect takes into account the effect of screening by the inner-shell electron which increases the effective charge seen by the electron lowering the binding energy.

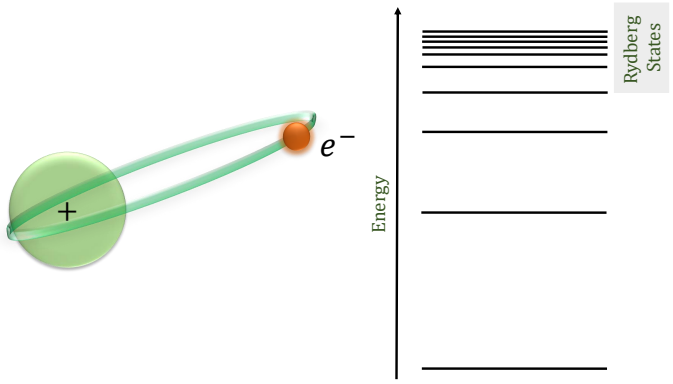

Figure 2.1: **a)** Electron in an orbit of very high radius (classical) and **b)** Energy series of Rydberg atom, Rydberg states are very closely spaced (quantum)

2.1.1 Interactions

Interatomic interactions are the most significant feature of Rydberg atoms. There are types of interaction regimes shown by Rydberg atoms depending on the separation between the atoms; dipole-dipole interaction and Van der Waal interaction. Dipole-dipole interaction is given by $V_{dipole} = \frac{C_3}{R^3}$ with $C_3 \propto (n-\delta_{njl})^4$, while van der Waal interaction goes as $V_{VdW} = \frac{C_6}{R^6}$ with $C_6 \propto (n-\delta_{njl})^{11}$. At a particular distance the interaction regime can be tuned properly around Foster resonance. The interaction explained here can lead to a very interesting many-body phenomena. It is known as Rydberg blockade where excitation of one atom prevents the excitation of a second atom under the effect of a field.

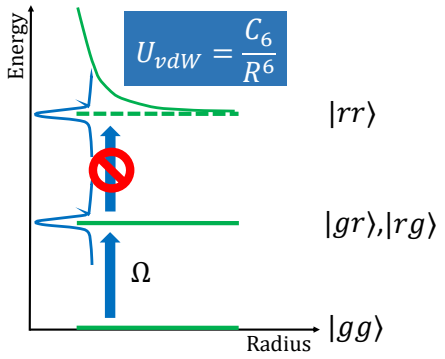

Figure 2.2: Rydberg blockade between two atoms in the van der Waals regime. The state $|rr\rangle$ is off resonant for the field due to U_{vdW}, this leads to the formation of the entangled state

In considering the van der Waal interaction regime, the energy of the state $|rr\rangle$ gets shifted by V_{VdW} and thus it gets decoupled. For two atoms, the state prepared under the blockade effect is entangled ($|\psi_+\rangle = \frac{|rg\rangle+|gr\rangle}{\sqrt{2}}$) and it is coupled to $|gg\rangle$ with Rabi frequncy $\sqrt{2}\Omega$. The state $|\psi_-\rangle = \frac{|rg\rangle-|gr\rangle}{\sqrt{2}}$ is not coupled to $|gg\rangle$. It is beacuse the total dipole is zero w.r.t that state i.e. $\langle gg|\,\hat{D}\,|\psi_-\rangle = 0$ with $\hat{D}$ as the dipole operator.

We can define a parameter named blockade radius (also called Condon radius) in an ensemble of atoms. Around any atom in Rydberg state a blockaded sphere is formed with radius R_b and inside this sphere no other excitations can exist.

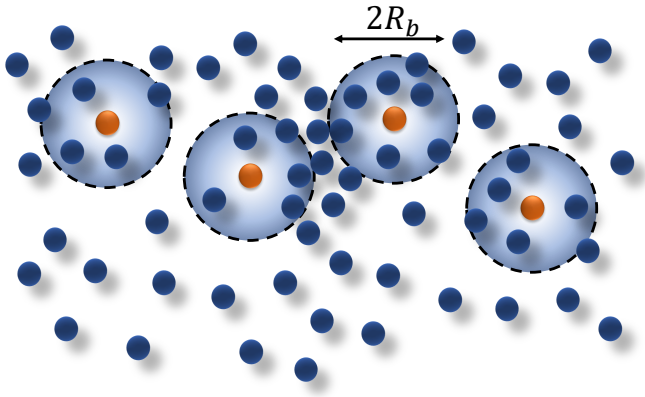

Figure 2.3: Blockade sphere around an atom in excited state of Radius R_b, there can not be a second excitation inside this sphere

This radius can be calculated very easily depending on the regime of interactions. In the Van der Waal interaction regime, $\hbar\Omega = \frac{C_6}{R_b^6} \Rightarrow R_b = \left\{\frac{C_6}{\hbar\Omega}\right\}^{\frac{1}{6}}$. We can define the blockade condition as $\Delta E = V_{VdW} > \hbar\Omega$ and we have applied this condition in reproducing basic results of blockade (details in the next chapter).

2.2 Photonic crystal waveguide

Photonic crystal can be considered as the optical analogue of atomic or molecular crystal lattice[39] which affects the motion of photons. In lattice we have a periodic potential along with atoms or molecules filling the sites, in case of photonic crystal we have periodic dielectric function, and electron's place is taken by photon. We are aware of band structures of crystal lattice. And there are band gaps which basically prohibits electron to move with certain energies. Photonic crystals can also be designed with photonic band gaps which prohibit

light from moving in certain directions with certain energies. This particular feature leads to a situation where flow of light can be molded. Thus photonic crystal has become an excellent tool to study light-matter interactions.

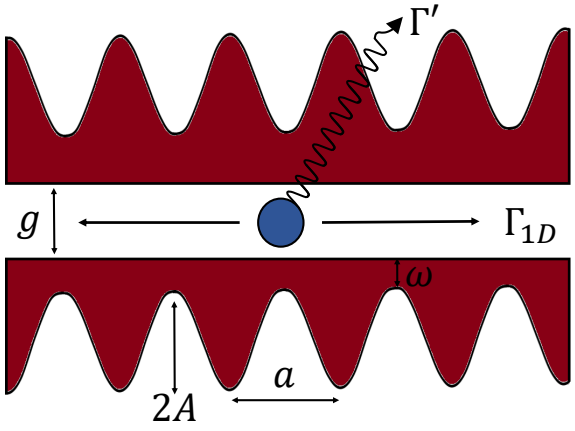

Figure 2.4: Alligator photonic crystal waveguide with an atom is trapped near it. Different structural parameters such as g: gap, a: periodicity, A: tooth amplitude of the edge and w: inner waveguide width determines the nature of the APCW. Guided mode plays an important role in the dynamics both in the coherent and dissipative regime.

The notion of photonic crystal becomes even more interesting when the idea of waveguide is merged with it. We can now think of quasi one-dimensional system which provides us guided modes inherently for a field. Experimental attempts have been made to study the physics of trapped atoms near photonic crystal. We have taken the advantage of many fruitful properties of this quasi-1D system in order understand the quantum dynamics of Rydberg atoms embedded to it. One of such properties is that near the photonic crystal if an imperfection is created then, a local cavity mode arises around that point. Trapping an atom can also be considered as an imperfection. Thus an array of trapped atom brings in different regime of interaction which pushes our system to a different level.

2.3 Quantum walk: An overview

The idea of quantum walk is at the heart of our project. It is basically the quantum analogue of classical random walk[40, 41, 42, 43, 44]. But quantum walk is inherently dictated by the fundamental aspects of quantum mechanics like superposition or interference. This makes it an interesting phenomenon to study. The outcome of quantum walk is very different from that of classical random walk as shown in figure 2.5.

Just like its classical analogue, there are two types of quantum walks - discrete-time quantum

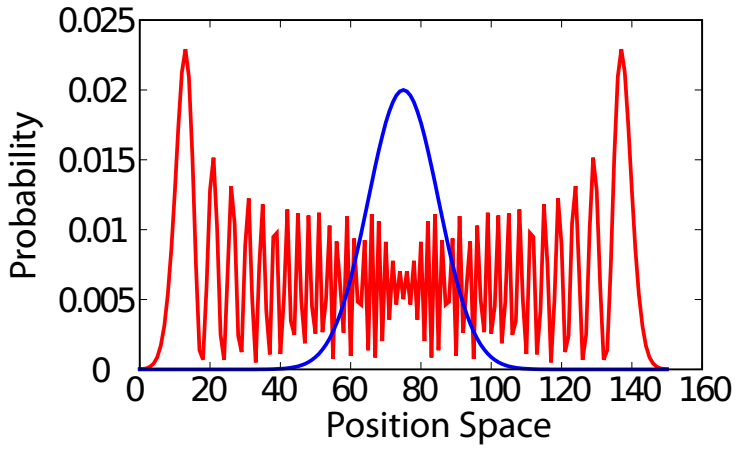

Figure 2.5: Probability of finding the walker at a certain position is plotted against the position space. Two cases- quantum (red) and classical-random (blue) walk show how different they are in nature

walk(DTQW) and continuous-time quantum walk(CTQW) [45]. We will give a brief overview of both of them.

2.3.1 Discrete-time quantum walk

In the case of discrete-time quantum walk (DTQW), the notion of coin operator comes into the picture, it dictates the direction of movement of the walker at each time-step. The action of coin operator is followed by a shift operator which drives the walker i.e. it makes it walk. Based on these two operators we can define a walk operator $\hat{Q}$. Mathematically $|\Psi(t)\rangle = \hat{Q}^t |\Psi(0)\rangle$ with $\hat{Q} = S(C \otimes \mathbb{1})$, S as shift and C as coin operator(written in the basis $\{|0\rangle, |1\rangle\}$). The form of the operators are given below

$$C = \begin{pmatrix} \cos\theta & -\mathrm{i}\sin\theta \\ -\mathrm{i}\sin\theta & \cos\theta \end{pmatrix} \tag{2.2}$$

$$S = |0\rangle\langle 0| \otimes \sum_{j \epsilon Z} |\psi_{j-1}\rangle\langle\psi_j| + |1\rangle\langle 1| \otimes \sum_{j \epsilon Z} |\psi_{j+1}\rangle\langle\psi_j| \tag{2.3}$$

The state $|0\rangle$ and $|1\rangle$ indicates the direction of the walker at a particular time step. These two states can be associated with the internal states of the walker. For example, the eigen-vector of the Pauli spin matrices[46] can be used for this purpose.

The main advantage of DTQW is that the coin operator can be tuned to favour the system in hand. The study of DTQW has shown its connection to relativistic quantum mechanics

[47], along with neutrino oscillation[48].

2.3.2 Continuous-time quantum walk

The continuous-time quantum walk(CTQW)[49] is different conceptually although the expected probability distribution is same as the DTQW. We have to understand the classical version of continuous-time walk first in order to understand the quantum version of the walk which takes place entirely in the position space. For a one-dimensional system[50], the expected probability distribution in position space is given below.

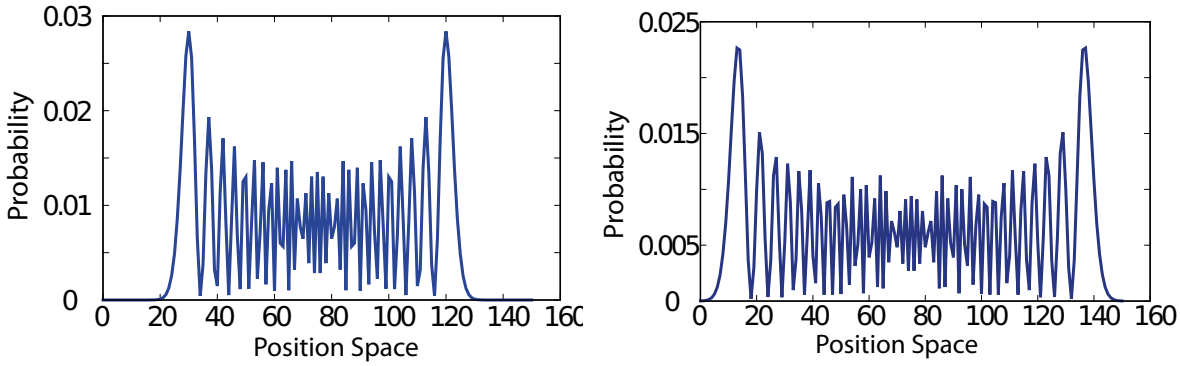

Figure 2.6: The probability distribution in position space of continuous-time quantum walker at two different instances of time(the figure in right is at a time later to the figure in left).

We can get a better understanding with the help of a graph which portrays a solid base of the dynamics. As shown in the figure below, the vertex set W with edge set F constitute the graph Q i.e. Q = (W, F). The position space H_p spanned by W and E.

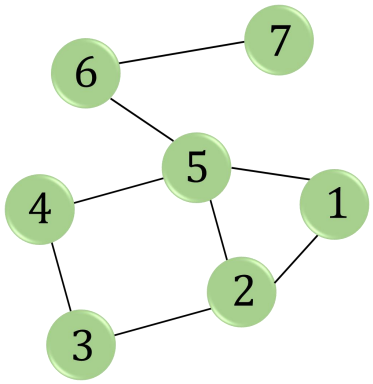

Figure 2.7: A graph Q with 7 vertices(W) and 8 edges(F)

The probability distribution goes through the vertices, along the edges giving rise to random walk. And the process can be formulated in terms of B as,

$$B_{j,k} = \begin{cases} 1, & \text{if } (j,k)\epsilon E \\ 0, & \text{otherwise} \end{cases} \tag{2.4}$$

Now by introducing rate of diffusion and degree of the vertices, we can define an important matrix associated with the graph Q. This is called the generator matrix H given by

$$H_{j,k} = \begin{cases} b_j\eta, & j = k \\ -\eta, & (j,k)\epsilon E \\ 0, & otherwise \end{cases} \tag{2.5}$$

Here η is the probability transition rate between nearest neighbours and b_j is the degree of the vertex j. The generator H drives the dynamics of the walker i.e. diffusion in graph G.

If $P_j(t)$ denotes the probability of being at vertex j at time t then the transition on graph G can be obtained as

$$\frac{d}{dt}P_j(t) = \sum_{k\epsilon V} H_{j,k}P_k(t) \tag{2.6}$$

The solution of the differential equation is given by

$$P(t) = e^{-\mathrm{i}Ht}P(0) \tag{2.7}$$

So far we have got an idea about the dynamics of continuous-time classical random walk. Now moving on to the quantum analogue of it, we can quantise the differential equation (2.6) which will bring quantum nature. By replacing the probabilities by the quantum amplitudes $c_j(t) = \langle j|\Psi(t)\rangle$ and introducing the factor i we get

$$\mathrm{i}\frac{d}{dt}c_j(t) = \sum_{k\epsilon V} H_{j,k}c_k(t) \tag{2.8}$$

It has similarities with the Schrodinger equation as

$$\mathrm{i}\frac{d}{dt}\left|\Psi\right\rangle = H\left|\Psi\right\rangle \tag{2.9}$$

The Hamiltonian is constructed keeping the rate generator matrix in mind (classical case) and it has to replicate the inherent nature of random walk in quantum case also.

To implement the simplest form of continuous-time quantum walk, CTQW on a line, the position Hilbert space H_p can be written as a state spanned by the basis states $|j\rangle$, where $j\epsilon Z$. The Hamiltonian H is defined such that

$$H|j\rangle = -\eta|j-1\rangle + 2\eta|j\rangle - \eta|j+1\rangle \tag{2.10}$$

In one-dimension continuous-time quantum walk is simply a finite difference Schrodinger equation

$$\mathrm{i}\frac{dc_j(t)}{dt} = -\eta[c_{j+1}(t) - 2c_j(t) + c_{j-1}(t)] \tag{2.11}$$

Here $c_j(t)$ are complex amplitudes at the (continuous) time and (discrete) lattice spacing j.

We now need to form a set up which can make the walker diffuse or hop around in the one-dimensional system. We have to make sure that such hopping is restricted only to nearest neighbour at each instances and photonic crystal waveguide provides that luxury to implement the system.

There are many ways we can see the benefits of the study on CTQW. Recently attempts have been made to explain photosynthetic energy transfer, using CTQW[51]. Moreover quantum version of travelling sales man problem has also been approached by using the notion of CTQW.

2.4 Summary

This chapter instills the fundamental concepts which are to used in the next few chapters. We discuss different parts of the system we use to emulate quantum walk dynamics in details. Special importance is given to explain the foundations of quantum walk. Although we are interested in continuous-time quantum walk, but we also discuss discrete-time quantum walk briefly.

Chapter 3

Rydberg excitation dynamics in optical lattice

In this chapter we study the dynamics of a two level atom with the excited state being the Rydberg state. We start with the single atom under an external field and understand how the population of the ground and the excited states change with time in non-dissipative case. We then incorporate dissipation into the two-level system. After understanding the single atom system, we introduce one more atom to the system. This is the part where Rydberg-Rydberg becomes crucial. We compare the change in the dynamics under the blockade condition with the single excitation case. The next section is about expressing number of excitations as a function of detuning. We discuss it for four atoms under near zero Rabi frequency condition.

3.1 Single atom dynamics

We started our work by verifying a few fundamental aspects of light-matter interaction for single two-level atom. At first it is done without decay and later with the inclusion of dissipation. The dynamics is given by the Jayne-Cummings Hamiltonian and under RWA it is given by $H = -\hbar\Delta + \frac{\hbar\Omega}{2}[\sigma_{eg} + \sigma_{ge}]$. Now the general state of the atom can be written as $|\psi\rangle = c_g |g\rangle + c_e |e\rangle$, and we numerically studied the dynamics of this state in terms of population of $|g\rangle$ and $|e\rangle$.

3.1.1 Without dissipation

The time evolution of the coefficients c_g and c_e can be written based on the above Hamiltonian as below. The dynamics is basically Rabi oscillation between $|g\rangle$ and $|e\rangle$ which is tuned by Δ and Ω. Moreover, we use $\tilde{c_e}$ in stead of c_e and $\tilde{c_e} = c_e e^{i\omega_0 t}$.

$$\dot{c_g} = -i\frac{\Omega}{2}\tilde{c_e} \tag{3.1}$$

$$\dot{\tilde{c_e}} = i\Delta\tilde{c_e} - i\frac{\Omega}{2}c_g \tag{3.2}$$

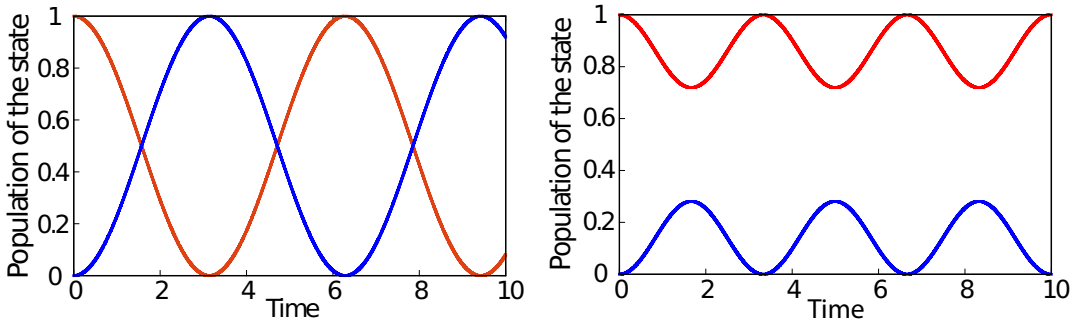

Figure 3.1: Rabi oscillation between the states $|g\rangle$ and $|e\rangle$ for (a) zero and (b) non-zero detuning

From the figure 3.1, we conclude that the amplitude of Rabi oscillation gets modified as Δ is changed.

3.1.2 With dissipation

To incorporate dissipative effect into dynamics (spontaneous emission), we have to solve quantum master equation. It can be written as

$$\partial_t \rho = -\frac{i}{\hbar}[H, \rho] + L_{decay}[\rho] \tag{3.3}$$

where ρ is the density matrix, H is the atomic Hamiltonian and $L_{decay}[\rho]$ is the Lindblad super operator and it is given as $L_{decay}[\rho] = L_\gamma[\rho] + L_\kappa[\rho]$ with spontaneous decay rate γ and cavity decay rate κ. The individual decay expression can be written as

$$L_\gamma[\rho] = -\frac{\gamma}{2}(\{\sigma_{ee}^j, \rho\} - 2\sigma_{ge}^j \rho \sigma_{eg}^j) \tag{3.4}$$

$$L_\kappa[\rho] = -\frac{\kappa}{2}(\{\hat{a}^\dagger \hat{a}_k, \rho\} - 2\hat{a}_k \rho \hat{a}_k^\dagger) \tag{3.5}$$

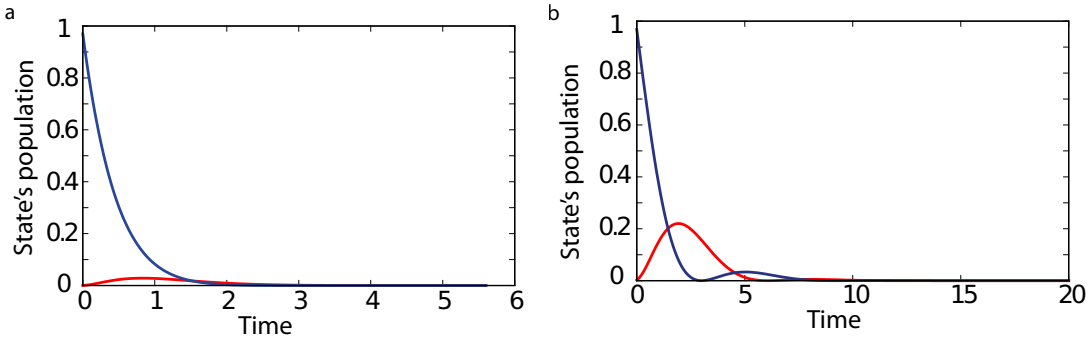

Figure 3.2: Here we have plotted the probabilities $|\rho_g(t)|$ (red solid line) and $|\rho_e(t)|$ (blue solid line) for an atom with initial state $\rho_g(0) = 0$ and $\rho_e(0)$=1. Figure (a) shows **intermediate coupling regime**; resonant case with parameters $(\Delta, \Omega, \gamma = \kappa)$= (0, 2.8, 3). Figure (b) shows **Strong coupling regime** under resonant case with parameters $(\Delta, \Omega, \gamma = \kappa)$=(0,10 ,3)

From figure 3.2, it can be concluded that when the coupling strength is strong, the Rabi oscillation lasts for longer time compared to weaker coupling strength.

3.2 Collective many-body dynamics

When an atomic ensemble is considered in such a way that the spatial dimension is less than the Rydberg blockade radius only one excitation is possible in the ensemble. Thus we get two states $|G\rangle = |ggg...g\rangle$ and $|R\rangle = \frac{1}{\sqrt{N}}[|rgg...g\rangle + |grg...g\rangle + ... + |ggg...r\rangle]$. The state $|R\rangle$ is superposition of all of the single excitation state. We want to show that the Rabi oscillation between the states $|G\rangle$ and $|R\rangle$ has an effective frequency $\sqrt{N}$ times more than that for single atom under the same field[52]. The Hamiltonian is composed of two parts - atomic and interaction Hamiltonian, $H = -\hbar\Delta \sum_{i=1}^{N} \sigma_{ee}^{(i)} + \frac{\hbar\Omega}{2} \sum_{i=1}^{N} [\sigma_{eg}^{(i)} + \sigma_{ge}^{(i)}]$. Thus, under the blockade condition a general state can be written as, $|\psi\rangle = c_G |G\rangle + c_R |R\rangle$. The time dependence of the coefficients can be written from Schrodinger equation (See in Appendix A) and we get

$$\dot{c_G} = -i\frac{\sqrt{N}\Omega}{2}c_R \tag{3.6}$$

$$\dot{c_R} = i\Delta c_R - i\frac{\sqrt{N}\Omega}{2}c_G \tag{3.7}$$

Comparing the above two equations with the equations 2.2 and 2.3 for single atoms, we can clearly see that the system under blockade condition has an effective Rabi frequency, $\Omega_{eff} = \sqrt{N}\Omega$. This shows the power of bloackade condition, which makes the ensemble behave like a superatom. We have numerically studied the blockade effect in an atomic chain of two atoms placed in a cavity through optical lattice. The Rabi oscillation is observed between the states $|gg\rangle$ and $\frac{1}{2}\{|gr\rangle + |rg\rangle\}$. By comparing the population of single atomic states and collective many-body states, the modification of Rabi frequency can be easily spotted.

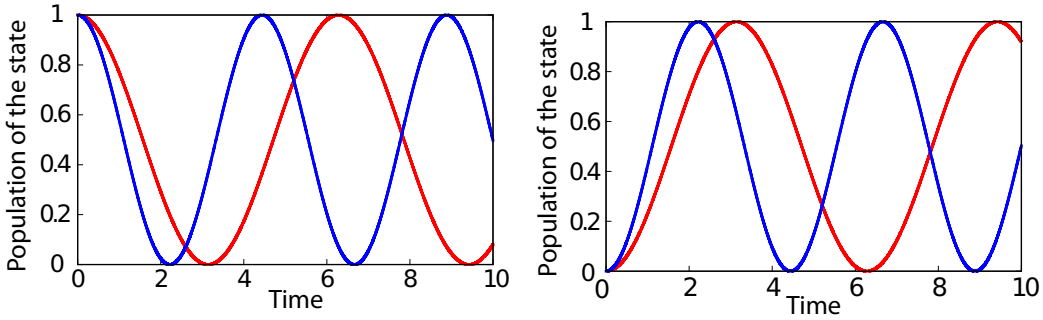

Figure 3.3: Comparison of population of (a) $|gg\rangle$(blue line) with $|g\rangle$(red line) and (b) $\frac{1}{2}\{|gr\rangle + |rg\rangle\}$(blue line) with $|e\rangle$(red line). We can clearly see the increase in the frequency of the collective states

Here, we limit ourselves to the non-dissipative part only as we are interested in the coherent dynamics the atomic chain.

3.3 Dynamical crystallisation: Controlled generation of Rydberg excitations

So far we have discussed in detail about the properties of Rydberg atom. It has one more significant aspect, the excitation of Rydberg atoms can generated in a controlled manner

which is called dynamical crystallisation.

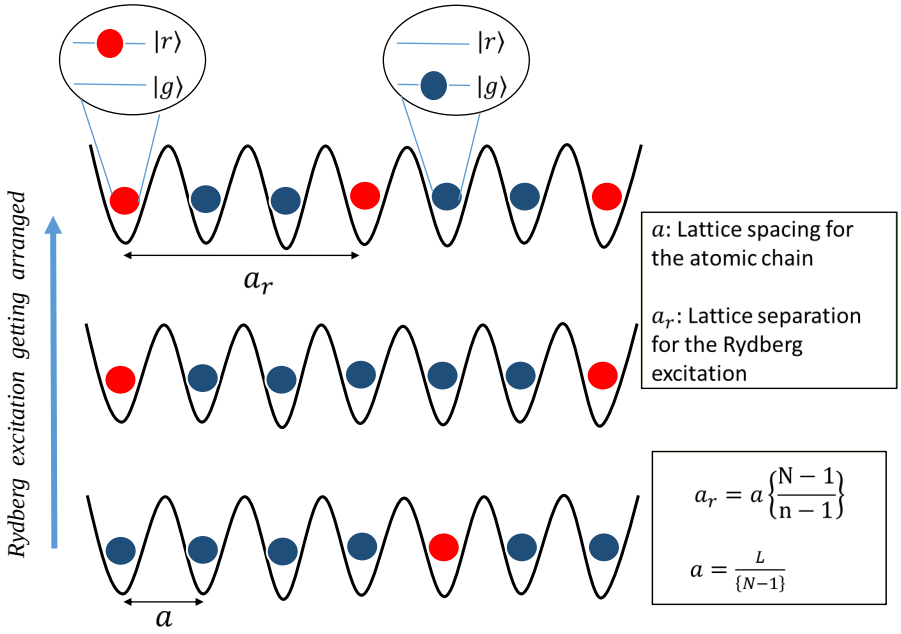

Figure 3.4: Depending on the number of Rydberg excitations, they are getting arranged in such a way that the interaction energy is minimum. Thus a crystal of Rydberg excitations is formed.

In near zero external field i.e. $\Omega \approx 0$, the number of Rydberg excitation can be obtained as a function of Detuning. The Hamiltonian in such case can be written as

$$H = -\hbar\Delta \sum_{i=1}^{N} \sigma_{ee}^{(i)} + \frac{C_6}{a^6} \sum_{i>j}^{N} \frac{\sigma_{ee}^{(i)} \sigma_{ee}^{(j)}}{(i-j)^6} \tag{3.8}$$

$$\tilde{H} = -\tilde{\Delta} \sum_{i=1}^{N} \sigma_{ee}^{(i)} + \sum_{i>j}^{N} \frac{\sigma_{ee}^{(i)} \sigma_{ee}^{(j)}}{(i-j)^6} \tag{3.9}$$

Here, $\tilde{\Delta} = \frac{\hbar a^6}{C_6}\Delta$ and $\tilde{H} = \frac{a^6}{C_6}H$ with a as lattice spacing. Thus we see that $\tilde{H}$ depends linearly on $\tilde{\Delta}$, thus the energy versus detuning plot is a straight line. Here calculation is made for the state with minimum energy w.r.t a particular number of Rydberg excitation.

We can deduce this easily for N atoms i.e. we will have 2^N different possible states. For

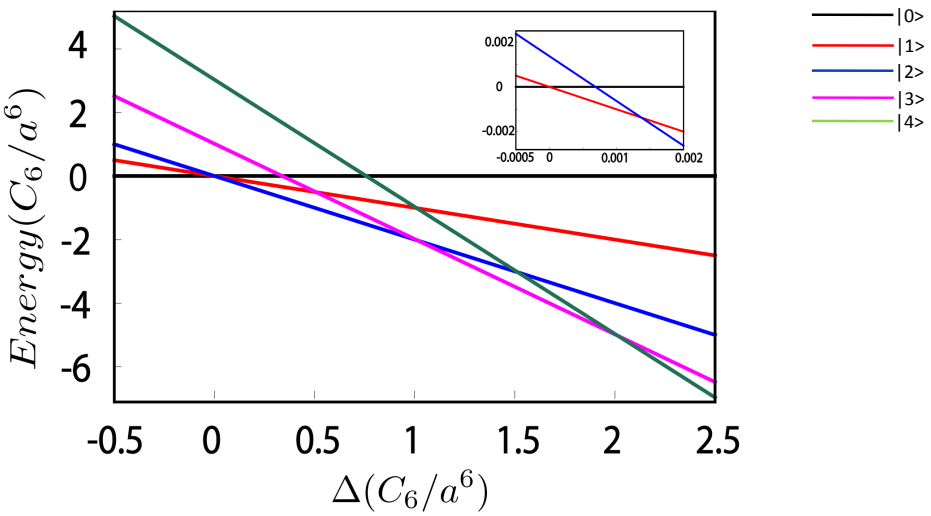

Figure 3.5: Energy versus detuing plot for the states with zero (black), one (red), two (blue), three (pink) and four (green) excitations for N=4 atoms. **Inset**: It is showing the difference amongst the point of intersections for zero, one and two excitations

N atoms, single excitation state can be any of the N different single-excited states, so they are all degenerate. The energy of a singly-excited state can be written as $E^{(1)}_{min} = -\Delta$. Considering the two excitations configuration, the one where two excitations are separated by maximum distance will be of lowest energy, and the energy can be calculated as $E^{(2)}_{min} = -2\Delta + \frac{C_6}{(N-1)^6 a^6}$. For three excitation configuration, there are two ways the lowest energy states can be evaluated. If N is an odd number, then the configuration with two of the excitations on each end (1st and Nth position) of the atomic chain with the third excitation on exact middle position ($\frac{N+1}{2}$th) will give rise to lowest energy configuration. The energy can be calculated as $E^{(3)}_{min} = -3\Delta + \frac{C_6}{(N-1)^6 a^6} + \frac{2C_6}{(\frac{N-1}{2})^6 a^6}$. We can find approximately the minimum energy of a configuration with n excitation[53], and it is given as

$$E^{(n)}_{min} = -n\Delta + \frac{C_6(n-1)^6}{(N-1)^6 a^6} + \sum_{j=1}^{n-1} \frac{j}{(n-j)^6}$$
$$E^{(n)}_{min} \approx -n\Delta + \frac{C_6(n-1)^7}{(N-1)^6 a^6} \tag{3.10}$$

As the number of excitation increases, the approach to find the configuration with lowest energy becomes non-trivial. The approach taken above is a very crude way to understand the

differences of configuration w.r.t a particular number of Rydberg excitations. But it can be understood in a much more systematic way[27] which highlights the potential of many-body states.

Let's assume that we have an atomic chain of length L consisting N atoms. The atomic separation or the lattice constant is given as $b = \frac{L}{N-1}$. Considering zero Rabi frequency, we can move from atomic to excitation manifold. If n is the number of excitation in a configuration, then there are $\binom{N}{n}$ profiles with n excitation and the one with lowest energy is of utmost interest. In the excitation manifold of n excitations, the lowest energy state pushes the separation between two excitation to a maximum value, which is given as $b_n = \frac{L}{n-1}$. Thereby a crystal of Rydberg excitation is formed. We will assume that excitation number is relatively smaller i.e. $b_n >> b$. Thus the energy of the configuration with n excitations can be written as,

$$E_n = -n\Delta + (n-1)\frac{C_6}{b_n^6} \tag{3.11}$$

$$E_n = -n\Delta + (n-1)^7\frac{C_6}{L^6} \tag{3.12}$$

Let Δ_{n+1}^n be the detuning at which the system makes a transition from n-excitations to (n+1)-excitations manifold. It can obtained as $E_{n+1} = E_n \Rightarrow \Delta_{n+1}^n = \{n^7 - (n-1)^7\}\frac{C_6}{L^6}$. Now Considering $n >> 1$, we can write,

$$\Delta_{n+1}^n = 7\frac{C_6}{L^6}n^6 \tag{3.13}$$

The above equation helps in determining the density of Rydberg excitation along with the Rydberg atom lattice spacing. So far no laser intensity is considered; when a laser is brought into the picture then the whole scenario becomes dynamically different. Laser excitation causes transition between crystal states and lifts the degeneracy of a manifold.

3.4 Summary

The primary idea to study single atom dynamics is to get an idea about the interaction of light with two-level system. This helps us to understand the role of Δ and Ω (comes from the term $\bar{d}.\bar{E}$ in the dipole interaction term of the atom under the field $\bar{E}$). We study the single

atom dynamics for constant Rabi frequency by changing the detuning. However it can also be studied for time-varying case which gives interesting dynamics which we chose to ignore as our system doesn't contain such interaction. The study of dynamical crystallisation helps us to find out a parameter to to decide the number of excitation at given time. As we were interested in single excitation case in a cavity at the initial phase of our work, thus getting an idea about the detuning value to generate such coonfigurations was very important.

Chapter 4

Coherent dynamics in photonic crystal waveguide

In this chapter we discuss the non-dissipative effect that arises in an atomic system trapped in photonic crystal waveguide. Section 4.1 deals with the Jaynes-Cummings model and how it can be mapped onto a system trapped in APCW. We discuss and derive the Hamiltonian of our system from fundamental interaction between atoms and photonic modes in section 4.2. Later we derive the length parameter which dictates the coherent dynamics in the waveguide. Finally, we express the Hamiltonian in terms of the dyadic Green's function as it embodies the inherent bloch profile of photonic crystal.

4.1 Alligator photonic crystal waveguide

We use a system where a one-dimensional array of atoms is embedded to an alligator photonic crystal waveguide (APCW). The array of atoms can be obtained by using an optical lattice or in the presence of substantial Casimir– Polder (CP) forces in photonic crystal waveguide[54, 55], thereby bringing periodicity to the system.

Spatial complexity of a system coupled to photonic crystal can be used as a tool to understand controlled dynamics. To understand this we discuss the dynamics of an atomic system in cavity. We know that, Jaynes-Cummings model describe the dynamics and the form of the

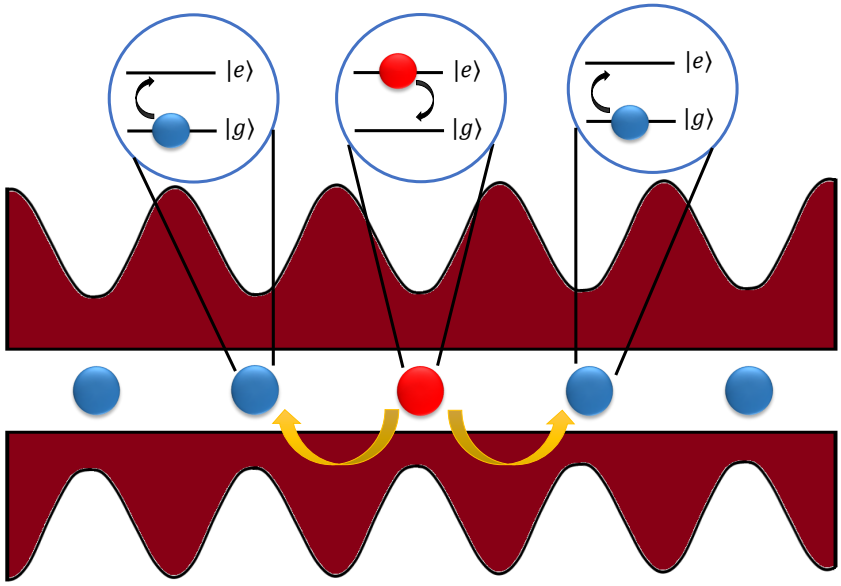

Figure 4.1: A schematic showing the coherent dynamics of an atomic chain (two-level scheme) embedded to **APCW**. For a single excitation configuration (an atom is excited by using an external field and after that field is switched off), the excited atom (red) then exchanges its excitation with the nearest-neighbour(tuned) atoms which are in ground state(blue).

Hamiltonian for a single atom in cavity is

$$H_{one-atom} = \hbar\omega_c \hat{a}^\dagger \hat{a} + \hbar\sigma_{ee} + \hbar g(\sigma_{eg}\hat{a} + \sigma_{ge}\hat{a}^\dagger) \tag{4.1}$$

In absence of the cavity field, $|e\rangle$ and $|g\rangle$ are the eigenstates of the atomic Hamiltonian. But they no longer are the eigenstates of the Hamiltonian H when the atom is placed in a cavity as the interaction between the cavity and the atom shifts the energies. The new eigenstates are, $|\psi_+\rangle = \cos(\theta)\,|e\rangle\,|0\rangle + \sin(\theta)\,|g\rangle\,|1\rangle$ and $|\psi_-\rangle = -\sin(\theta)\,|e\rangle\,|0\rangle + \cos(\theta)\,|g\rangle\,|1\rangle$. If cavity mode and atomic resonance frequency is highly detuned, it drastically changes the population of the respective states and modes. It can be explained by the mixing angle θ which determines the population on either state , $\theta = \frac{g_c}{\Delta_c}$. Under this condition, $\theta << 1$ as $\Delta_c = \omega_a - \omega_c >> g_c$. From the expression of $|\psi_+\rangle$, it's quite clear that the atomic excitation dominates the photonic component. Now, if we introduce another atom in the cavity with ground state configuration, the second atom exchanges the excitation of the first

atom. Thus in an atomic chain, the excitation hops around the chain in the cavity. This additional interaction is given by[56]

$$H_I^{ef-cavity} = \frac{g_c^2}{\Delta_c} \sum_{j,l} \sigma_{eg}^j \sigma_{ge}^l \tag{4.2}$$

Clearly the above effective interaction Hamiltonian has no spatial dpendence. Despite the lack of spatial dependence it leads to some interesting phenomena.[57, 58, 59, 60]. Now, if we replace cavity with alligator photonic crystal waveguide, while keeping the rest of the parameters intact, we obtain a similar excitation exchange along the atomic chain. The excitation will be delocalised over the photonic degrees of freedom as

$$|1\rangle = \int dk c_k^* \hat{a}_k |0\rangle \tag{4.3}$$

Moreover, the photonic crystal will modify the effective interaction as

$$H_I = \frac{g^2}{2\Delta} \sum_{j,l} f(z_j, z_l) \sigma_{eg}^j \sigma_{ge}^l \tag{4.4}$$

4.2 The Hamiltonian of the system

In interaction picture the interaction between the atom and photonic crystal modes is

$$H_I = \hbar \sum_{j=1}^{N} \int dk g_k \sigma_{eg}^j \hat{a}_k u_k(z_j) e^{i\delta_k t + ikz_j} + H.c \tag{4.5}$$

So the full Hamiltonian under RWA(w.r.t the atomic frequency ω_a) is given by

$$H = -\hbar \int dk \delta_k \hat{a}_k^\dagger \hat{a}_k + \hbar \sum_{j=1}^{N} \int dk [g_k \sigma_{eg}^j \hat{a}_k u_k(z_j) e^{ikz_j} + g_k \sigma_{ge}^j \hat{a}_k^\dagger u_k^*(z_j) e^{-ikz_j}] \tag{4.6}$$

On the other hand the dissipative dynamics is contained in the equation

$$L[\rho] = -\frac{\gamma}{2} \sum (\{\sigma_{ee}^j, \rho\} - 2\sigma_{ge}^j \rho \sigma_{eg}^j) - \frac{\kappa}{2} \int dk (\{\hat{a}^\dagger \hat{a}_k, \rho\} - 2\hat{a}_k \rho \hat{a}_k^\dagger) \tag{4.7}$$

The dynamics of the photonic modes depend on the dynamics of creation($\hat{a}_k^\dagger$) and annihilation($\hat{a}_k$) operator. So we derive the rate equation for these operators from Heisenberg equation of motion. Rate of change of coherent part of $\hat{a}_k$ is derived as

$$\dot{\hat{a}}_k = \frac{i}{\hbar}[H, \hat{a}_k] \tag{4.8}$$

$$\dot{\hat{a}}_k = \frac{i}{\hbar}[-\hbar \int dk' \delta_{k'} \hat{a}_{k'}^\dagger \hat{a}_{k'} + \hbar \sum_{j=1}^{N} \int dk' (g\sigma_{eg}^j \hat{a}_{k'} u_{k'}(z_j) e^{ik'z_j} + g\hat{a}_{k'}^\dagger \sigma_{ge}^j u_{k'}^*(z_j) e^{-ik'z_j}), \hat{a}_k] \tag{4.9}$$

$$\dot{\hat{a}}_k = i[-\int dk' \delta_{k'} \hat{a}_{k'}^\dagger \hat{a}_{k'}, \hat{a}_k] + ig[\sum_{j=1}^{N} \int dk' (g\sigma_{eg}^j \hat{a}_{k'} u_{k'}(z_j) e^{ik'z_j} + g\hat{a}_{k'}^\dagger \sigma_{ge}^j u_{k'}^*(z_j) e^{-ik'z_j}), \hat{a}_k] \tag{4.10}$$

$$\dot{\hat{a}}_k = -i \int dk' \delta_{k'} [\hat{a}_{k'}^\dagger \hat{a}_{k'}, \hat{a}_k] + ig \sum_{j=1}^{N} \int dk' [(\sigma_{eg}^j \hat{a}_{k'} u_{k'}(z_j) e^{ik'z_j} + \hat{a}_{k'}^\dagger \sigma_{ge}^j u_{k'}^*(z_j) e^{-ik'z_j}), \hat{a}_k] \tag{4.11}$$

$$\dot{\hat{a}}_k = -i \int dk' \delta_{k'} (-\delta(k - k')) \hat{a}_{k'} + ig \sum_{j=1}^{N} \int dk' \{u_{k'}(z_j) e^{ik'z_j} \sigma_{eg}^j [\hat{a}_{k'}, \hat{a}_k] + u_{k'}^*(z_j) e^{-ik'z_j}) [\hat{a}_{k'}^\dagger, \hat{a}_k] \sigma_{ge}^j\} \tag{4.12}$$

$$\dot{\hat{a}}_k = i\delta_k \hat{a}_k - ig \sum_{j=1}^{N} \{u_k^*(z_j) e^{-ikz_j}\} \sigma_{ge}^j \tag{4.13}$$

Now introducing dissipation into the system, we get (full rate equation)

$$\dot{\hat{a}}_k = (i\delta_k - \frac{\kappa}{2}) \hat{a}_k - ig \sum_{j=1}^{N} \{u_k^*(z_j) e^{-ikz_j}\} \sigma_{ge}^j \tag{4.14}$$

Considering $\gamma << \kappa$ and $g << min\{\delta_k, \kappa\}$, the photonic modes can be adiabatically elimi-

nated.the field operator takes the form

$$\dot{\hat{a}}_k = 0 \longrightarrow \hat{a}_k = \frac{g\sum_{j=1}^{N}\{u_k^*(z_j)e^{-ikz_j}\}\sigma_{ge}^j}{(\delta_k + i\frac{\kappa}{2})} \tag{4.15}$$

$$\hat{a}_k = \frac{g(\delta_k - i\frac{\kappa}{2})\sum_{j=1}^{N}\{u_k^*(z_j)e^{-ikz_j}\}\sigma_{ge}^j}{\delta_k^2 + \frac{\kappa^2}{4}} \tag{4.16}$$

Putting this expression back into the Hamiltonian (eq. 4.6), we get

$$\begin{aligned} H = -\hbar\int dk\delta_k(\frac{g(\delta_k + i\frac{\kappa}{2})\sum_{i=1}^{N}\{u_k(z_i)e^{ikz_i}\}\sigma_{eg}^i}{\delta_k^2 + \frac{\kappa^2}{4}})(\frac{g(\delta_k - i\frac{\kappa}{2})\sum_{j=1}^{N}\{u_k^*(z_j)e^{-ikz_j}\}\sigma_{ge}^j}{\delta_k^2 + \frac{\kappa^2}{4}}) + \\ \hbar\sum_{j=1}^{N}\int dk[g\sigma_{eg}^j(\frac{g(\delta_k - i\frac{\kappa}{2})\sum_{j=1}^{N}\{u_k^*(z_j)e^{-ikz_j}\}\sigma_{ge}^j}{\delta_k^2 + \frac{\kappa^2}{4}})u_k(z_j)e^{ikz_j} \\ +g\sigma_{ge}^j(\frac{g(\delta_k + i\frac{\kappa}{2})\sum_{i=1}^{N}\{u_k(z_i)e^{ikz_i}\}\sigma_{eg}^i}{\delta_k^2 + \frac{\kappa^2}{4}})u_k^*(z_j)e^{-ikz_j}] \end{aligned} \tag{4.17}$$

$$\begin{aligned} H = -\hbar g^2\sum_{i,j}\sigma_{eg}^i\sigma_{ge}^j\int dk\frac{\delta_k u_k(z_i)u_k^*(z_j)e^{ik(z_i - z_j)}}{\delta_k^2 + \frac{\kappa^2}{4}} \\ +\hbar g^2\sum_{i,j}\sigma_{eg}^i\sigma_{ge}^j\int dk[(\frac{(\delta_k - i\frac{\kappa}{2})u_k(z_i)u_k^*(z_j)e^{ik(z_i - z_j)}}{\delta_k^2 + \frac{\kappa^2}{4}}) \\ +(\frac{(\delta_k + i\frac{\kappa}{2})u_k(z_i)u_k^*(z_j)e^{ik(z_i - z_j)}}{\delta_k^2 + \frac{\kappa^2}{4}})] \end{aligned} \tag{4.18}$$

$$\begin{aligned} H = \hbar g^2\sum_{i,j}\sigma_{eg}^i\sigma_{ge}^j\int dk\{\frac{-\delta_k u_k(z_i)u_k^*(z_j)e^{ik(z_i - z_j)}}{\delta_k^2 + \frac{\kappa^2}{4}} + \\ \frac{(\delta_k - i\frac{\kappa}{2})u_k(z_i)u_k^*(z_j)e^{ik(z_i - z_j)}}{\delta_k^2 + \frac{\kappa^2}{4}} + \frac{(\delta_k + i\frac{\kappa}{2})u_k(z_i)u_k^*(z_j)e^{ik(z_i - z_j)}}{\delta_k^2 + \frac{\kappa^2}{4}}\} \end{aligned} \tag{4.19}$$

$$H = \hbar g^2 \sum_{i,j} \sigma_{eg}^i \sigma_{ge}^j \int dk \{ \frac{\delta_k u_k(z_i) u_k^*(z_j) e^{ik(z_i - z_j)}}{\delta_k^2 + \frac{\kappa^2}{4}} \}$$

As we know that, around the band edge wave-vector

$$\begin{aligned} E_k(z) &= e^{ikz} u_{k_0}(z) \\ E_k(z) &= e^{i(k-k_0)z} E_{k_0}(z) \end{aligned} \tag{4.20}$$

Thus we can write that

$$H = \hbar g^2 \sum_{i,j} \sigma_{eg}^i \sigma_{ge}^j \int dk \{ \frac{\delta_k E_k(z_i) E_k^*(z_j)}{\delta_k^2 + \frac{\kappa^2}{4}} \}$$

Applying the quadratic approximation around the band edge $\omega_k = \omega_b(1 - \alpha(k - k_0)^2/k_0^2)$ where α is the band curvature and writing $\Delta = \omega_a - \omega_b$, we get

$$H = \hbar g^2 \sum_{i,j} \sigma_{eg}^j \sigma_{ge}^i E_{k_0}(z_j) E_{k_0}^*(z_i) \int dk \frac{\delta_k e^{i(k-k_0)(z_i - z_j)}}{\delta_k^2 + (\kappa/2)^2} \tag{4.21}$$

After solving this integral (the process of integration is given in Appendix A), we end up with the Hamiltonian

$$H = \frac{g_c^2}{2\Delta} \sum_{i,j} E_{k_0}(z_i) E_{k_0}^*(z_j) e^{-|z_i - z_j|/L} \sigma_{eg}^i \sigma_{ge}^j \tag{4.22}$$

where $g_c = g\sqrt{2\pi/L}$ and thus we can see the emergence of spatially modulated interaction here. This is the Hamiltonian of our system, an atomic chain of Rydberg of atoms embedded to APCW. The Hamiltonian can be obtained by using Nakajima-Zwanzig approach also (see in Appendix A).

4.3 Determining the length parameter

The length parameter L plays the most important part in controlling the nature of dynamics. We know that L is given as

$$L = \sqrt{\frac{\alpha\omega_b}{\Delta k_0^2}} \tag{4.23}$$

Thus we see that L depends on inherent nature of the photonic crystal like α - band curvature[61, 38]

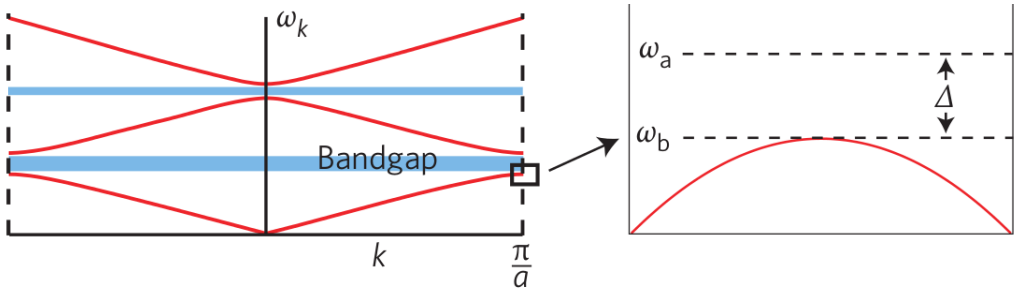

Figure 4.2: Band structure of 1D photonic crystal, here guided mode frequency ω_k is plotted against Bloch wave-vector k in the first Brillouin zone
. **Courtesy**: Figure taken from [62]

Moreover the detuning Δ plays the role of the parameter which tunes the length parameter. We emulate the signature quantum walk distribution along with the linear dependence of spread on time for L values around $0.5a$ (a is the lattice constant of APCW).

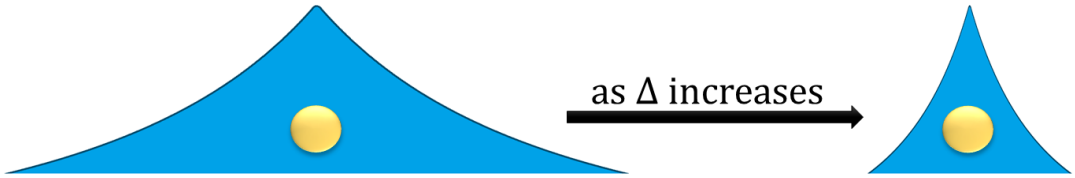

Figure 4.3: It reflects how the detuning change the photonic envelope around the atomic position and along with the effective cavity length.

As L depends on band curvature, band edge frequency and wave-vector, so tuning can be made w.r.t to the detuning only. So Δ has to be chosen appropriately although it will be very high. In case of alligator photonic crystal waveguide, α=10.6, $\frac{\omega_b}{2\pi}$=333 THz, $k_0 = \pi/a$, thus we get $L = 0.5a \Rightarrow \frac{\alpha\omega_b}{\Delta\pi^2} = 0.25$, and we arrive at $\Delta = \frac{4\alpha\omega_b}{\pi^2}$. Thus we find that the detuning to get nearest neighbour exchange is very high and in case of APCW, $\Delta \approx 1430.56$ THz.

4.4 The Green's function approach

To incorporate the role of the bloch modes that appear in the Hamiltonian, we use the dyadic Green's function approach[63], which comes from the response of the atoms in photonic crystal waveguide. Considering APCW, a quasi-1D nanostructure, the full Green tensor (or function) can be written as $G(r_i, r_j, \omega_a) = G_{1D}(r_i, r_j, \omega_a) + G\prime(r_i, r_j, \omega_a)$, where G_{1D} corresponds to the guided mode along the waveguide mediating atom-atom interactions and $G\prime$ is the contribution from all of the other modes (includes decay effect). As we work in the band gap regime of the photonic crystal waveguide, hence we can directly use the guided portion of the Green function[63]. Thus the Green's function takes the form,

$$G(r_i, r_j, \omega_a) = G_{1D}(r_i, r_j, \omega_a) = (J_{1D} + i\frac{\Gamma_{1D}}{2})cos(\frac{\pi r_i}{a})\cos(\frac{\pi r_j}{a})exp[-|r_i - r_j|/L] \quad (4.24)$$

But for a relatively long photonic crystal waveguide, Γ_{1D} is negligible i.e. $\Gamma_{1D} \approx 0$. This is because the photonic envelope is highly localised, thereby preventing dissipation through the guided mode. Finally, the Green's function can be written as,

$$G(r_i, r_j, \omega_a) = J_{1D}\cos(\frac{\pi r_i}{a})\cos(\frac{\pi r_j}{a})exp[-|r_i - r_j|/L] \quad (4.25)$$

For cavity, the coefficient J_{1D} is given as $J_{1D}^{cavity} = \frac{-g_c^2\Delta_c}{\Delta_c^2+\kappa_c^2/4}$. The physics of the atoms embedded to PCW can be mapped onto the similar system in a cavity. In this case we can define the factor J_{1D} for PCW as well by introducing the map, $g_c \longrightarrow \bar{g_c}$ and $\Delta_c \longrightarrow \bar{\Delta}_c$. Thus for an atomic chain coupled to photonic crystal waveguide,

$$J_{1D} = \frac{-\bar{g_c}^2\bar{\Delta}_c}{\bar{\Delta_c}^2 + \bar{\kappa_c}^2/4} \quad (4.26)$$

We have here $\bar{\Delta}_c = 2\Delta$ (as $\delta = \Delta$) and $\bar{\kappa_c} = \kappa$, thus $J_{1D} = \frac{-\bar{g_c}^2(2\Delta)^2)}{(2\Delta)^2+\kappa^2/4}$ Now neglecting terms in the second order of (κ/Δ) as we work in a higher detuning regime, we get $J_{1D} = \frac{-\bar{g_c}^2}{2\Delta}$.. As $g_c = 2\pi(12.2\sqrt{a/L})GHz$, we can write the Green's function as

$$G(r_i, r_j, \omega_a) = \frac{-\bar{g_c}^2}{2\Delta}\cos(\frac{\pi r_i}{a})\cos(\frac{\pi r_j}{a})exp[-|r_i - r_j|/L] \quad (4.27)$$

$$G(r_i, r_j, \omega_a) = \frac{-61.9827 \times 10^6}{\sqrt{\Delta}} \cos(\frac{\pi r_i}{a}) \cos(\frac{\pi r_j}{a}) exp[-|r_i - r_j|/L] \tag{4.28}$$

In terms of the Green function, the Hamiltonian[64] can be written in the band gap regime as

$$H = -\mu_0 \omega_a^2 \sum_{i,j}^{N} \{d.^* ReG(r_i, r_j, \omega_a).d\} \sigma_{eg}^i \sigma_{ge}^j \tag{4.29}$$

$$H = -\frac{3\pi\hbar\mu_0\epsilon_0\omega_a^3}{3\pi\hbar\epsilon_0\omega_a} \sum_{i,j}^{N} \{d.^* ReG(r_i, r_j, \omega_a).d\} \sigma_{eg}^i \sigma_{ge}^j \tag{4.30}$$

$$H = -\{\frac{\omega_a^3 |d|^2}{3\pi\hbar\epsilon_0\omega_a^3}\}\{\frac{3\hbar\pi c}{\omega_a}\} \sum_{i,j}^{N} ReG(r_i, r_j, \omega_a) \sigma_{eg}^i \sigma_{ge}^j \tag{4.31}$$

$$H = -\gamma_0\{\frac{3\hbar\pi c}{\omega_a}\} \sum_{i,j}^{N} ReG(r_i, r_j, \omega_a) \sigma_{eg}^i \sigma_{ge}^j \tag{4.32}$$

Here $\gamma_0 = \frac{\omega_a^3 |d|^2}{3\pi\hbar\epsilon_0\omega_a^3}$ is the free space emission rate. After putting the expression for the Green's function, the Hamiltonian takes the form

$$H = \gamma_0\{\frac{3\hbar\pi c}{\omega_a}\} \frac{61.9827 \times 10^6}{\sqrt{\Delta}} \sum_{i,j}^{N} \cos(\frac{\pi r_i}{a}) \cos(\frac{\pi r_j}{a}) exp[-|r_i - r_j|/L] \sigma_{eg}^i \sigma_{ge}^j \tag{4.33}$$

$$\frac{H}{\gamma_0\hbar} = \{\frac{3\pi \times 3 \times 10^8}{\omega_b + \Delta}\} \frac{61.9827 \times 10^6}{\sqrt{\Delta}} \sum_{i,j}^{N} \cos(\frac{\pi r_i}{a}) \cos(\frac{\pi r_j}{a}) exp[-|r_i - r_j|/L] \sigma_{eg}^i \sigma_{ge}^j \tag{4.34}$$

$$\frac{H}{\gamma_0\hbar} = \Big\{\frac{1.75 \times 10^5}{(2092.3 + \Delta)\sqrt{\Delta}}\Big\} \sum_{i,j}^{N} \{\cos(\frac{\pi r_i}{a}) \cos(\frac{\pi r_j}{a}) exp[-|r_i - r_j|/L]\} \sigma_{eg}^i \sigma_{ge}^j \tag{4.35}$$

The cos terms appear in the Hamiltonian are the profiles of the Bloch modes. This term brings a chiral impact on the dynamics.

4.5 Summary

In this chapter we go through the derivation of the Hamiltonian in two ways to eliminate the photonic modes. The length parameter is crucial which leads us to quantum walk dynamics. We discuss the range of detuning in order to obtain the nearest neighbour excitation ex-

change. In the Hamiltonian, there are terms showing the profile of the bloch modes, thus to incorporate the effect of bloch modes, we look into our system in Green's function formalism. We express the interaction Hamiltonian in terms of Green's function. We carefully choose a regime in band structure, as the Green's function has dissipative part in non-band gap regime. We work in the band gap regime to get coherent dynamics.

Chapter 5

Single excitation: Quantum walk dynamics

In this chapter we discuss the results we have for single excitation coherent dynamics. Section 5.1 deals with the probability distribution of the excitation on the atomic chain. We discuss it for 101 and 151 atoms considering a symmetric and an asymmetric initial condition. We explain how the results resemble the quantum walk dynamics. In section 5.2 we calculate the spread of the excitation over the atomic chain and determines its dependence on time. We explain the importance of time factor for a certain atomic chain.

5.1 Distribution of the excitation on the atomic chain

The probability of finding the excitation at a position can be obtained by taking the projection of the wave function on the position space. Single excitation is very easy to map onto the position space as the position is very similar to the configuration used in the numerical study. The study is for nearest neighbour exchange, thus we tune the length parameter to a value half of the atomic separation in the chain i.e. $L = 0.5a$. For single excitation case, we are considering an atomic chain with odd number of atoms, N=101 and 151.

5.1.1 Symmetric Initial Condition

In this case initial position of the excitation is at the $\frac{N-1}{2}$th site in the atomic chain, where N is the number of atoms in the chain.

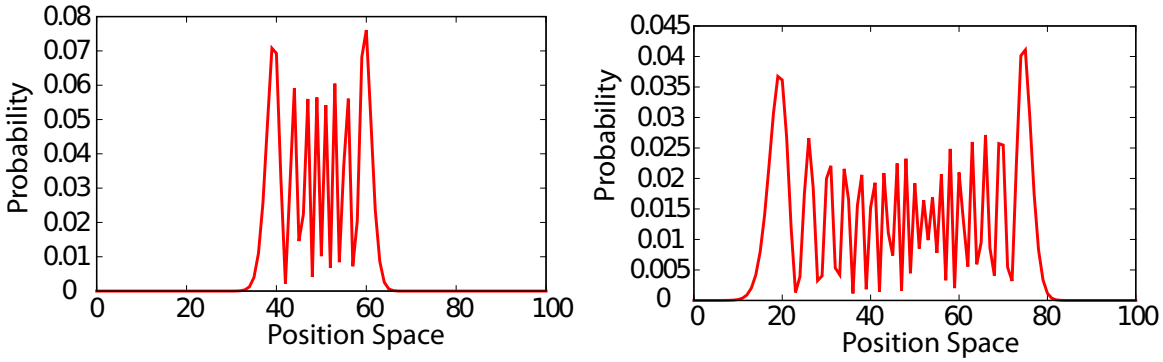

Figure 5.1: Showing the distribution of the excitation on the position in two different instances of time (figure in the right side corresponds to a larger time than the figure in the left side)for a case where the atom is at 50th site of the atomic chain initially i.e. symmetric initial condition. The atomic chain have 101 atoms here.

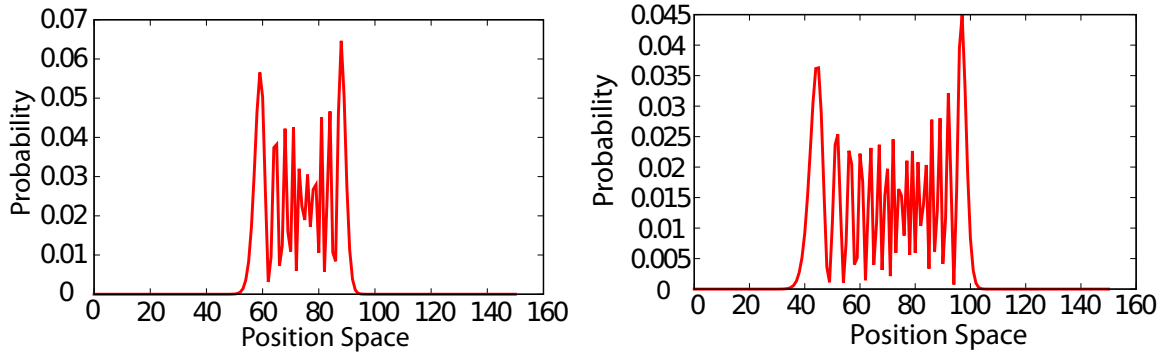

Figure 5.2: Showing the distribution of the excitation on the position in two different instances of time (figure in the right side corresponds to a larger than the figure in the left side) for a case where the atom is at 75th site of the atomic chain initially i.e. for symmetric initial case. The atomic chain have 151 atoms here.

We can clearly see here that the height of peak towards the end of an atomic chain in the figure 5.1 and figure 5.2 is more along a particular direction. This can be termed as a chiral behaviour where a certain direction is preferred over the other in the waveguide (i.e. the atomic chain).

5.1.2 Asymmetric initial condition

If we change the change the initial condition to an asymmetric one i.e. the excitation is at a site other than the $\frac{N-1}{2}$th site initially. This implies that the time taken by the excitation to reach one end of the chain different from the time taken to reach the other end.

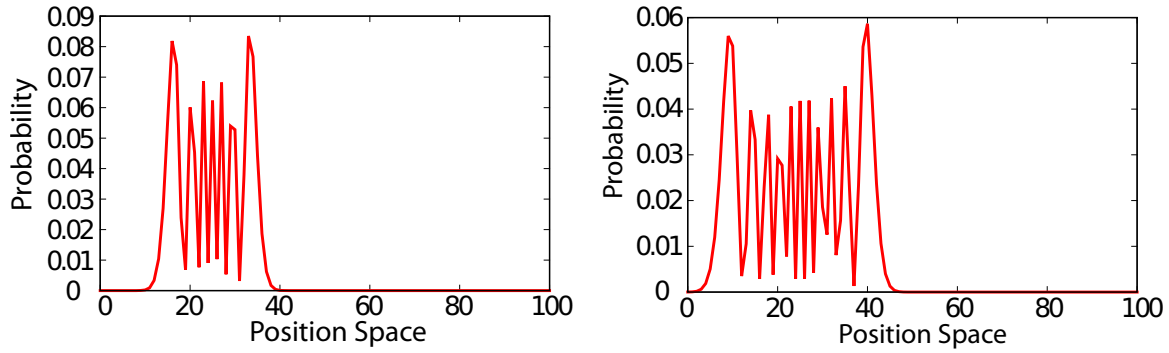

Figure 5.3: Showing the distribution of the excitation on the position in two different instances of time (figure in the right side corresponds to a larger than the figure in the left side) for a case where the atom is at 25th site of the atomic chain initially i.e. for asymmetric initial case. The atomic chain have 101 atoms here.

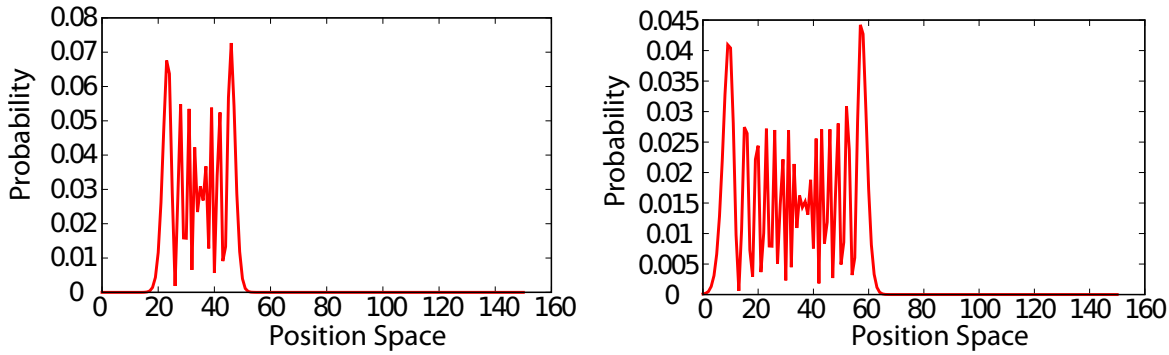

Figure 5.4: Showing the distribution of the excitation on the position in two different instances of time (figure in the right side corresponds to a larger than the figure in the left side) for a case where the atom is at 35th site of the atomic chain initially i.e. for asymmetric initial case. The atomic chain have 151 atoms here.

From figure 5.3 and figure 5.4, it can be seen that probability distribution is heavier towards the end, from where the initial position of the excitation is the closest. Thus from both of the initial conditions, we see the similarity of the plots with figure 2.6 and it states that the excitation hopping along the atomic chain is similar to the quantum walk dynamics with excitation as the walker.

5.2 Description of the spread

This is the crucial result for our system as it shows when the excitation is behaving like a quantum walker. It determines the time up to which quantum walk dynamics persists. We know that for classical random walk spread(standard deviation) goes as $\sqrt{time}$ while in quantum walk that is linear w.r.t time. And we get exactly the linear plot but the linearity disappears after the excitation reaches either side of the atomic chain. We focused on the linear part, where excitation shows quantum walk like dynamics.

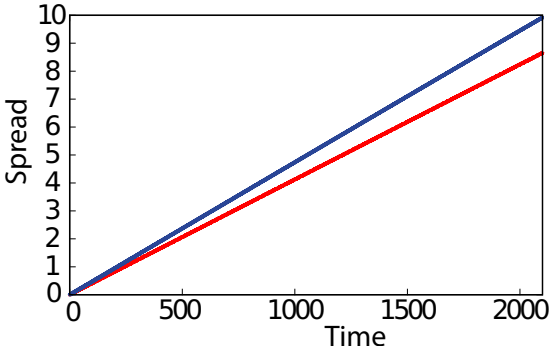

Figure 5.5: Comparing the spread of the the two cases differed by initial condition. The *blue* line is for asymmetric initial condition where the excitation is at 25th site of the atomic and the *red* line is for the one with excitation's initial position at the 50th site i.e. symmetric case. The atomic chain have 101 atoms

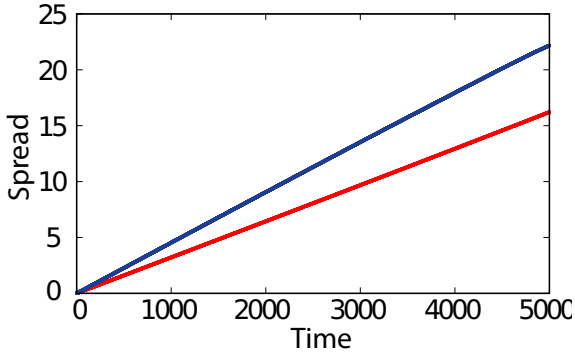

Figure 5.6: Comparing the spread of the the two cases differed by initial condition. The *blue* line is for asymmetric initial condition where the excitation is at 35th site of the atomic and the *red* line is for the one with excitation's initial position at the 75th site i.e. symmetric case. The atomic chain have 151 atoms

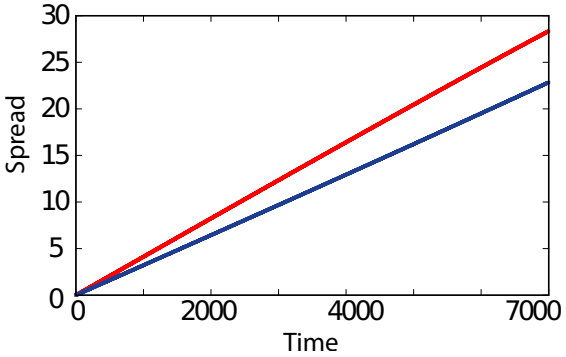

Figure 5.7: Comparing the spread of the the two cases differed by length of the atomic chains. The *blue* line is for N=101 atoms and the *red* line is for N=151 atoms with symmetric initial condition in both cases

We can clearly see that the spread of the excitation i.e. quantum walker depends on the initial condition. In other words, the slope of the spread versus time plot is determined by the initial position of the excitation on the atomic chain. The slope of the plot for asymmetric initial condition is higher than that of symmetric initial condition. It implies that the spread of the excitation over the position space is much faster for asymmetric case. Moreover, the length of the atomic chain does affect the spread of the excitation. For a symmetric initial condition, the slope of the plot for 101 atoms is more than that of 151 atoms. Shorter atomic chain corresponds to faster spread.

5.3 Summary

We discussed briefly about the outcome of single excitation dynamics when projected to position space, we see that it is quite similar to the signature quantum walk plot shown in the first chapter. Our claim is supported by the spread versus time plot, which shows linear behaviour. The important part of this linear plot is that its slope shows a particular pattern w.r.t number of atoms. Moreover the linearity vanishes after sometime signalling that the walker has reached the boundary and no more quantum walk dynamics persists, thereby making time-factor a significant part of our system. We study the dynamics for atomic chains with different number of atoms to understand the effect of length of the atomic chain on the dynamics.

Chapter 6

Conclusion and Outlook

In this chapter, we summarise our results briefly and discuss the future directions of our work. In chapter 2, we give importance to the basic concepts like Rydberg atoms, photonic crystal etc. which are used in chapter 3 and chapter 4. Chapter 3 is about the dynamics of Rydberg atoms under an external field, and we are working on such a system embedded to photonic crystal waveguide where Rydberg-Rydberg interactions play a handy role. Chapter 4 is totally dedicated to the set up we use to study the coherent dynamics of the atomic chain. In chapter 5, we discuss the results of our study of single excitation dynamics. The result obtained has shown similarities with expected plots of quantum walk dynamics. And the spread of the walker goes linearly with time. Thus single excitation manifold under the exchange gives us quantum walk dynamics.

There are many questions still need to be investigated. For example, we can study the dynamics of double excitations i.e. double quantum walker. It will be really interesting to see how the interatomic interactions will modify the dynamics. Moreover, we have plans to get the dynamics for a general case i.e n excitations. We can study in details the chiral character of photonic crystal waveguide in coherent regime.

Moreover, we can also incorporate the effects of the environment on the quantum walker. There are two regimes we can explore - Markovian and non-Markovian regime. Depending on the strength of the system-environment interactions one regime dominates the other. In the non-Markovian regime, we can tune the dynamics of the quantum walker in such a way that it can emulate localised behaviour. All these aspects of an atomic system embedded to photonic crystal waveguide make it a very exciting field to study.

Bibliography

[1] Michael A Nielsen and Isaac L Chuang. *Quantum computation and Quantum information*. Cambridge University Press India, 2000.

[2] John Preskill. Lecture notes for physics 229: Quantum information and computation. *California Institute of Technology*, 16, 1998.

[3] L-M Duan, MD Lukin, J Ignacio Cirac, and Peter Zoller. Long-distance quantum communication with atomic ensembles and linear optics. *Nature*, 414(6862):413–418, 2001.

[4] Peter Komar, Eric M Kessler, Michael Bishof, Liang Jiang, Anders S Sørensen, Jun Ye, and Mikhail D Lukin. A quantum network of clocks. *Nature Physics*, 10(8):582–587, 2014.

[5] H Jeff Kimble. The quantum internet. *Nature*, 453(7198):1023–1030, 2008.

[6] Andrew D Greentree, Charles Tahan, Jared H Cole, and Lloyd CL Hollenberg. Quantum phase transitions of light. *Nature Physics*, 2(12):856–861, 2006.

[7] Michael J Hartmann, Fernando GSL Brandao, and Martin B Plenio. Strongly interacting polaritons in coupled arrays of cavities. *Nature Physics*, 2(12):849–855, 2006.

[8] Dimitris G Angelakis, Marcelo Franca Santos, and Sougato Bose. Photon-blockade-induced mott transitions and x y spin models in coupled cavity arrays. *Physical Review A*, 76(3):031805, 2007.

[9] Seth Lloyd. Universal quantum simulators. *Science*, 273(5278):1073, 1996.

[10] Antonio Acín, J Ignacio Cirac, and Maciej Lewenstein. Entanglement percolation in quantum networks. *Nature Physics*, 3(4):256–259, 2007.

[11] Daniel A Steck. Quantum and atom optics. *Oregon Center for Optics and Department of Physics, University of Oregon*, page 47, 2007.

[12] Edward Mills Purcell. Spontaneous emission probabilities at radio frequencies. In *Confined Electrons and Photons*, pages 839–839. Springer, 1995.

[13] Daniel Kleppner. Inhibited spontaneous emission. *Physical Review Letters*, 47(4):233, 1981.

[14] Serge Haroche and Daniel Kleppner. Cavity quantum electrodynamics. *Physics Today*, 42(1):24–30, 1989.

[15] Peter Lodahl, Sahand Mahmoodian, and Søren Stobbe. Interfacing single photons and single quantum dots with photonic nanostructures. *Reviews of Modern Physics*, 87(2):347, 2015.

[16] G Epple, KS Kleinbach, TG Euser, NY Joly, T Pfau, P St J Russell, and R Löw. Rydberg atoms in hollow-core photonic crystal fibres. *Nature communications*, 5, 2014.

[17] Peter Lodahl, Sahand Mahmoodian, Søren Stobbe, Philipp Schneeweiss, Jürgen Volz, Arno Rauschenbeutel, Hannes Pichler, and Peter Zoller. Chiral quantum optics. *arXiv preprint arXiv:1608.00446*, 2016.

[18] Crispin Gardiner and Peter Zoller. The quantum world of ultra-cold atoms and light. 2014.

[19] Crispin Gardiner and Peter Zoller. The quantum world of ultra-cold atoms and light book ii: The physics of quantum-optical devices. In *The Quantum World of Ultra-Cold Atoms and Light Book II: The Physics of Quantum-Optical Devices*, pages 1–524. World Scientific, 2015.

[20] Akihisa Goban. *Strong atom-light interactions along nanostructures: Transition from free-space to nanophotonic interfaces*. 2015.

[21] R Mitsch, C Sayrin, B Albrecht, P Schneeweiss, and A Rauschenbeutel. Quantum state-controlled directional spontaneous emission of photons into a nanophotonic waveguide. *Nature communications*, 5, 2014.

[22] Hannes Pichler, Tomás Ramos, Andrew J Daley, and Peter Zoller. Quantum optics of chiral spin networks. *Physical Review A*, 91(4):042116, 2015.

[23] Mark Saffman, Thad G Walker, and Klaus Mølmer. Quantum information with rydberg atoms. *Reviews of Modern Physics*, 82(3):2313, 2010.

[24] MD Lukin, M Fleischhauer, R Cote, LM Duan, D Jaksch, JI Cirac, and P Zoller. Dipole blockade and quantum information processing in mesoscopic atomic ensembles. *Physical Review Letters*, 87(3):037901, 2001.

[25] E Urban, Todd A Johnson, T Henage, L Isenhower, DD Yavuz, TG Walker, and M Saffman. Observation of rydberg blockade between two atoms. *Nature Physics*, 5(2):110–114, 2009.

[26] Alpha Gaëtan, Yevhen Miroshnychenko, Tatjana Wilk, Amodsen Chotia, Matthieu Viteau, Daniel Comparat, Pierre Pillet, Antoine Browaeys, Philippe Grangier, et al. Observation of collective excitation of two individual atoms in the rydberg blockade regime. *Nature Physics*, 5(2):115–118, 2009.

[27] T Pohl, E Demler, and Mikhail D Lukin. Dynamical crystallization in the dipole blockade of ultracold atoms. *Physical review letters*, 104(4):043002, 2010.

[28] Hendrik Weimer, Robert Löw, Tilman Pfau, and Hans Peter Büchler. Quantum critical behavior in strongly interacting rydberg gases. *Physical Review Letters*, 101(25):250601, 2008.

[29] Robert Löw, Hendrik Weimer, Ulrich Krohn, Rolf Heidemann, Vera Bendkowsky, Björn Butscher, Hans Peter Büchler, and Tilman Pfau. Universal scaling in a strongly interacting rydberg gas. *Physical Review A*, 80(3):033422, 2009.

[30] Hendrik Weimer and Hans Peter Büchler. Two-stage melting in systems of strongly interacting rydberg atoms. *Physical review letters*, 105(23):230403, 2010.

[31] B Olmos, R González-Férez, and I Lesanovsky. Fermionic collective excitations in a lattice gas of rydberg atoms. *Physical review letters*, 103(18):185302, 2009.

[32] S Ji, C Ates, and I Lesanovsky. Two-dimensional rydberg gases and the quantum hard-squares model. *Physical review letters*, 107(6):060406, 2011.

[33] Igor Lesanovsky. Many-body spin interactions and the ground state of a dense rydberg lattice gas. *Physical review letters*, 106(2):025301, 2011.

[34] Galina Khitrova, HM Gibbs, M Kira, Stephan W Koch, and Axel Scherer. Vacuum rabi splitting in semiconductors. *Nature Physics*, 2(2):81–90, 2006.

[35] E Vetsch, D Reitz, G Sagué, R Schmidt, ST Dawkins, and A Rauschenbeutel. Optical interface created by laser-cooled atoms trapped in the evanescent field surrounding an optical nanofiber. *Physical review letters*, 104(20):203603, 2010.

[36] A Goban, KS Choi, DJ Alton, D Ding, C Lacroûte, M Pototschnig, T Thiele, NP Stern, and HJ Kimble. Demonstration of a state-insensitive, compensated nanofiber trap. *Physical Review Letters*, 109(3):033603, 2012.

[37] JD Thompson, TG Tiecke, NP de Leon, J Feist, AV Akimov, M Gullans, AS Zibrov, V Vuletić, and MD Lukin. Coupling a single trapped atom to a nanoscale optical cavity. *Science*, 340(6137):1202–1205, 2013.

[38] A Goban, C-L Hung, S-P Yu, JD Hood, JA Muniz, JH Lee, MJ Martin, AC McClung, KS Choi, Darrick E Chang, et al. Atom–light interactions in photonic crystals. *Nature communications*, 5, 2014.

[39] Joshua N. Winn John D. Joannopoulos, Robert David Meade. *Photonic Crystal*. Princeton University Press, 2016.

[40] Richard P Feynman, Albert R Hibbs, and Daniel F Styer. *Quantum mechanics and path integrals*. Courier Corporation, 2010.

[41] Yakir Aharonov, Luiz Davidovich, and Nicim Zagury. Quantum random walks. *Physical Review A*, 48(2):1687, 1993.

[42] Julia Kempe. Quantum random walks: an introductory overview. *Contemporary Physics*, 44(4):307–327, 2003.

[43] Robin Côté, Alexander Russell, Edward E Eyler, and Phillip L Gould. Quantum random walk with rydberg atoms in an optical lattice. *New Journal of Physics*, 8(8):156, 2006.

[44] Philipp M Preiss, Ruichao Ma, M Eric Tai, Alexander Lukin, Matthew Rispoli, Philip Zupancic, Yoav Lahini, Rajibul Islam, and Markus Greiner. Strongly correlated quantum walks in optical lattices. *Science*, 347(6227):1229–1233, 2015.

[45] Jingbo Wang and Kia Manouchehri. *Physical implementation of quantum walks*. Springer, 2013.

[46] CM Chandrashekar. Two-component dirac-like hamiltonian for generating quantum walk on one-, two-and three-dimensional lattices. *arXiv preprint arXiv:1309.3911*, 2013.

[47] Arindam Mallick and CM Chandrashekar. Dirac cellular automaton from split-step quantum walk. *Scientific reports*, 6, 2016.

[48] Arindam Mallick, Sanjoy Mandal, and CM Chandrashekar. Neutrino oscillations in discrete-time quantum walk framework. *The European Physical Journal C*, 77(2):85, 2017.

[49] Edward Farhi and Sam Gutmann. Quantum computation and decision trees. *Physical Review A*, 58(2):915, 1998.

[50] Chandrashekar Madaiah. Discrete-time quantum walk-dynamics and applications. 2010.

[51] Masoud Mohseni, Patrick Rebentrost, Seth Lloyd, and Alan Aspuru-Guzik. Environment-assisted quantum walks in photosynthetic energy transfer. *The Journal of chemical physics*, 129(17):11B603, 2008.

[52] YO Dudin, L Li, F Bariani, and A Kuzmich. Observation of coherent many-body rabi oscillations. *Nature Physics*, 8(11):790–794, 2012.

[53] David Petrosyan, Klaus Mølmer, and Michael Fleischhauer. On the adiabatic preparation of spatially-ordered rydberg excitations of atoms in a one-dimensional optical lattice by laser frequency sweeps. *Journal of Physics B: Atomic, Molecular and Optical Physics*, 49(8):084003, 2016.

[54] S-P Yu, JD Hood, JA Muniz, MJ Martin, Richard Norte, C-L Hung, Seán M Meenehan, Justin D Cohen, Oskar Painter, and HJ Kimble. Nanowire photonic crystal waveguides for single-atom trapping and strong light-matter interactions. *Applied Physics Letters*, 104(11):111103, 2014.

[55] CL Hung, SM Meenehan, DE Chang, O Painter, and HJ Kimble. Trapped atoms in one-dimensional photonic crystals. *New Journal of Physics*, 15(8):083026, 2013.

[56] GS Agarwal, S Dutta Gupta, and RR Puri. *Fundamentals of cavity quantum electrodynamics*. World Scientific, 1994.

[57] MB Plenio, SF Huelga, A Beige, and PL Knight. Cavity-loss-induced generation of entangled atoms. *Physical Review A*, 59(3):2468, 1999.

[58] Peter Domokos and Helmut Ritsch. Collective cooling and self-organization of atoms in a cavity. *Physical review letters*, 89(25):253003, 2002.

[59] Adam T Black, Hilton W Chan, and Vladan Vuletić. Observation of collective friction forces due to spatial self-organization of atoms: from rayleigh to bragg scattering. *Physical review letters*, 91(20):203001, 2003.

[60] Kristian Baumann, Christine Guerlin, Ferdinand Brennecke, and Tilman Esslinger. Dicke quantum phase transition with a superfluid gas in an optical cavity. *Nature*, 464(7293):1301–1306, 2010.

[61] Sajeev John and Jian Wang. Quantum electrodynamics near a photonic band gap: Photon bound states and dressed atoms. *Physical review letters*, 64(20):2418, 1990.

[62] James S Douglas, H Habibian, C-L Hung, AV Gorshkov, H Jeff Kimble, and Darrick E Chang. Quantum many-body models with cold atoms coupled to photonic crystals. *Nature Photonics*, 9(5):326–331, 2015.

[63] A Asenjo-Garcia, JD Hood, DE Chang, and HJ Kimble. Atom-light interactions in quasi-1d nanostructures: a green's function perspective. *arXiv preprint arXiv:1606.04977*, 2016.

[64] Marco T Manzoni, Darrick E Chang, and James S Douglas. Simulating quantum light propagation through atomic ensembles using matrix product states. *arXiv preprint arXiv:1702.05954*, 2017.

Appendices

Appendix A

Detail calculation

A.1 Calculation of collective many-body oscillation

$$i\hbar\frac{d}{dt}[c_G\left|G\right\rangle + c_R\left|R\right\rangle] = H[c_G\left|G\right\rangle + c_R\left|R\right\rangle] \tag{A.1}$$

$$i\hbar[\dot{c_G}\left|G\right\rangle + \dot{c_R}\left|R\right\rangle] = -\hbar\Delta\sum_{i=1}^{N}\sigma_{ee}^{(i)}[c_G\left|G\right\rangle + c_R\left|R\right\rangle] + \frac{\hbar\Omega}{2}\sum_{i=1}^{N}[\sigma_{eg}^{(i)} + \sigma_{ge}^{(i)}][[c_G\left|G\right\rangle + c_R\left|R\right\rangle] \tag{A.2}$$

$$\begin{aligned} &= -\hbar\Delta\sum_{i=1}^{N}\sigma_{ee}^{(i)}[c_G\left|G\right\rangle + c_R\frac{1}{\sqrt{N}}[\left|rgg...g\right\rangle + \left|grg...g\right\rangle + ... + \left|ggg...r\right\rangle]] \\ &+\frac{\hbar\Omega}{2}\sum_{i=1}^{N}[\sigma_{eg}^{(i)} + \sigma_{ge}^{(i)}][c_G\left|G\right\rangle + c_R\frac{1}{\sqrt{N}}[\left|rgg...g\right\rangle + \left|grg...g\right\rangle + ... + \left|ggg...r\right\rangle] \end{aligned} \tag{A.3}$$

$$\begin{aligned} &= -\hbar\Delta\frac{1}{\sqrt{N}}c_R\sum_{i=1}^{N}\sigma_{ee}^{(i)}[\left|rgg...g\right\rangle + \left|grg...g\right\rangle + ... + \left|ggg...r\right\rangle] \\ &+\frac{\hbar\Omega}{2}\sum_{i=1}^{N}\sigma_{eg}^{(i)}[c_G\left|G\right\rangle + c_R\frac{1}{\sqrt{N}}[\left|rgg...g\right\rangle + \left|grg...g\right\rangle + ... + \left|ggg...r\right\rangle]] \\ &+\frac{\hbar\Omega}{2}\sum_{i=1}^{N}\sigma_{ge}^{(i)}[c_G\left|G\right\rangle + c_R\frac{1}{\sqrt{N}}[\left|rgg...g\right\rangle + \left|grg...g\right\rangle + ... + \left|ggg...r\right\rangle]] \end{aligned} \tag{A.4}$$

$$= -\hbar\Delta\frac{1}{\sqrt{N}}c_R[|rgg...g\rangle + |grg...g\rangle + ... + |ggg...r\rangle]$$
$$+\frac{\hbar\Omega}{2}[c_G[|rgg...g\rangle + |grg...g\rangle + ... + |ggg...r\rangle] + c_R\frac{1}{\sqrt{N}}|X\rangle]$$
$$+\frac{\hbar\Omega}{2}c_R\frac{1}{\sqrt{N}}[|ggg...g\rangle + |ggg...g\rangle + ... + |ggg...g\rangle] \quad (A.5)$$

$$= -\hbar\Delta c_R|R\rangle + \frac{\hbar\Omega}{2}\sqrt{N}c_G|R\rangle + \frac{\hbar\Omega}{2}c_R\frac{1}{\sqrt{N}}|X\rangle + \frac{\hbar\Omega}{2}c_R\frac{1}{\sqrt{N}}[N|G\rangle] \quad (A.6)$$

Here $|X\rangle$ is none of the states $|G\rangle$ and $|R\rangle$ and it will get eliminated inherently in later stages of equation. Thus we have

$$i\hbar[\dot{c_G}|G\rangle + \dot{c_R}|R\rangle] = -\hbar\Delta c_R|R\rangle + \frac{\hbar\sqrt{N}\Omega}{2}c_G|R\rangle + \frac{\hbar\sqrt{N}\Omega}{2}c_R|G\rangle + \frac{\hbar\Omega}{2}c_R\frac{1}{\sqrt{N}}|X\rangle \quad (A.7)$$

Now multiplying the above equation by $\langle G|$ and $\langle R|$ separately we get two equations,

$$\dot{c_G} = -i\frac{\sqrt{N}\Omega}{2}c_R \quad (A.8)$$

$$\dot{c_R} = i\Delta c_R - i\frac{\sqrt{N}\Omega}{2}c_G \quad (A.9)$$

A.2 Solution of the integral appear in the Hamiltonian

$$H_I = \sum_{j,l}\sigma_{eg}^j\sigma_{ge}^l E_{k_0}(z_j)E_{k_0}^*(z_l)\int dk\frac{g_k^2\delta_k e^{i(k-k_0)(z_j-z_l)}}{\delta_k^2 + (\kappa/2)^2} \quad (A.10)$$

Clearly δ_k linearly depends on Δ and thus considering the terms only to the first order of κ/Δ we get-

$$H_I = \sum_{j,l}\sigma_{eg}^j\sigma_{ge}^l E_{k_0}(z_j)E_{k_0}^*(z_l)\int dk\frac{g_k^2 e^{i(k-k_0)(z_j-z_l)}}{\delta_k} \quad (A.11)$$

Considering coupling constant g_k to be invariant w.r.t field modes, we obtain

$$H_I = \sum_{j,l} \sigma_{eg}^j \sigma_{ge}^l E_{k_0}(z_j) E_{k_0}^*(z_l) g^2 \int dk \frac{e^{i(k-k_0)(z_j - z_l)}}{\Delta + \omega_b \alpha (k-k_0)^2 / k_0^2} \tag{A.12}$$

Now defining $L = \sqrt{\frac{\alpha \omega_b}{\Delta k_0^2}}$ and $p = k - k_0$

$$H_I = \sum_{j,l} \sigma_{eg}^j \sigma_{ge}^l E_{k_0}(z_j) E_{k_0}^*(z_l) \frac{g^2}{\Delta} \int dp \frac{e^{ip(z_j - z_l)}}{1 + p^2 L^2} \tag{A.13}$$

$$H_I = \sum_{j,l} \sigma_{eg}^j \sigma_{ge}^l E_{k_0}(z_j) E_{k_0}^*(z_l) \frac{g^2}{\Delta L^2} \int dp \frac{e^{ip(z_j - z_l)}}{(p + i/L)(p - i/L)} \tag{A.14}$$

Complex integration leads us to

$$H_I = \sum_{j,l} \sigma_{eg}^j \sigma_{ge}^l E_{k_0}(z_j) E_{k_0}^*(z_l) \frac{g^2}{\Delta L^2} 2\pi i \{ \frac{e^{-|z_j - z_l|/L}}{(2i/L)} \} \tag{A.15}$$

$$H_I = \sum_{j,l} \sigma_{eg}^j \sigma_{ge}^l E_{k_0}(z_j) E_{k_0}^*(z_l) \frac{\pi g^2}{\Delta L} e^{-|z_j - z_l|/L} \tag{A.16}$$

$$H_I = \frac{g_c^2}{2\Delta} \sum_{j,l} E_{k_0}(z_j) E_{k_0}^*(z_l) e^{-|z_j - z_l|/L} \sigma_{eg}^j \sigma_{ge}^l \tag{A.17}$$

where $g_c = g\sqrt{2\pi/L}$.

Appendix B

Description of techniques and approximation

B.1 Technique used

This is the key part of our work. Here we will explain how we emulate the physical system as a program. This part will contain three different sections, mainly detuning dependence of energy, Rabi oscillation under blockade effect and emulating quantum walk using single excitation.

We try to relate the notion of atomic chain to binary code as ground state($|g\rangle$) and excited state($|e\rangle$) is reflected by the digits **0** and **1** respectively. Thus for an atomic chain of 5 atoms the state $|eegeg\rangle$ is represented by the binary number **11010**. This helps us to relate each and every state to a decimal number and that decimal number contains informations about that particular state. We have a general algorithm to do so. If we consider N to be the number of atoms in the atomic chain, then there are 2^N possible states. So by using the index i=0,1,2,....,2^N-1 we can assign each and every state. Now we can extract information about the state by converting each and every number to its binary form. This binary form will tell us how many excited atoms are in a state along with the magnitude of interaction they possess.

This formalism helps us to determine the coupling of the atoms to cavity field or laser field with ease. More exchange of excitation can also be explained using this formalism very

easily.

B.2 Suzuki-Trotter decomposition

As time evolution is key to our work, thus we had to deal numerically with a lots of differential equation. And we have used split-operator technique to improve the accuracy of our results. We split the coefficient of a state to its real and imaginary part and these two parts are evolved at different way.

Let A and B be two operators, we know that Suzuki-Trotter decomposition of first order can be written as

$$e^{A+B} = \lim_{n\to\infty} \{e^{\frac{A}{n}} e^{\frac{B}{n}}\}^n \tag{B.1}$$

In the second the decomposition takes the form and we have used this particular order of Suzuki-Trotter decomposition

$$e^{A+B} = \lim_{n\to\infty} \{e^{\frac{A}{2n}} e^{\frac{B}{n}} e^{\frac{A}{2n}}\}^n \tag{B.2}$$

This numerical technique has played significantly important role in delivering accurate dynamics of our system.